Probing Atoms Using Scanning Tunnelling Microscopy

Thomas Coppell

200821131

BSc Project

Department of Physics

University of Liverpool

May 2020

Supervisor: H.R. Sharma/R. McGrath

Declaration:

I hereby declare that this thesis is my own work and effort and that it has not been submitted anywhere for any award. Where other sources of information have been used, they have been acknowledged.

– Thomas Coppell

Abstract

This thesis involves characterisation of the clean surface of the *i*-Ag-In-Yb quasicrystal and the thin film growth of Ag upon this surface. This is compared to theoretically derived results and previously published work. The clean surface of the quasicrystal is found to be consistent with both theoretical results and published work. The initial growth of Ag on the surface follows the theoretical work, but not as strongly as suggested, with much surface diffusion. The pentagon shaped growths are consistent with the theory, and compared to the previously published work of growing a thin film of Pb on the same quasicrystal. The side lengths of the pentagons formed by the Ag atoms were found to be 1.06±0.05 nm. The type of growth of Ag was characterised as Volmer-Weber.

Contents

1. Introduction

The aim of this project was the characterisation of the surface and thin film growth of Ag atoms on an icosahedral Ag-In-Yb quasicrystal. The results will be compared to previously published articles and theoretically derived results.

A quasicrystal is an aperiodically ordered structure[1]. Unlike periodic crystals; quasicrystals do not have translational symmetry. Whereas a periodic crystal can only have two-fold, three-fold, four-fold and six-fold rotational symmetries, quasicrystals can exhibit rotational symmetries that are forbidden in periodic crystals, such as five-fold and ten-fold rotational symmetry. This is exemplified by the diffraction pattern of quasicrystals which indicate these ‘forbidden’ rotational symmetries, and confirms their aperiodic nature. It was the observation of the ten-fold rotational symmetry of an aluminium and manganese alloy that led to the paper published by Dan Schechtmen in 1984 which established quasicrystals as an area of research in materials science.[1]

The surface characterisation of a quasicrystal is an important step in our understanding of them, and any potential applications: such as for coating materials, or use in catalysis.[2][3] This can be further simplified by growing a monoatomic thin film on the surface of the quasicrystal, as these epitaxial growths can reproduce the physical structure of the quasicrystal, with less chemical complexity. In this experiment, the characterisation of the surface of the quasicrystal and the thin film growth was done via low energy electron diffraction (LEED) and scanning tunnelling microscopy (STM). First, the clean surface was characterised with reference to a previously published paper “Structure of the fivefold surface of the Ag-In-Yb icosahedral quasicrystal”[4]. This involved finding the step heights between different terraces of the surface of the quasicrystal. Then, viewing a section of the surface through a fast Fourier transform filter, the aperiodic tiling was recreated, confirming the atomic structure expected from bulk termination. Next, images of the quasicrystal surface after 45 seconds of thin film growth were analysed. This was focused on the placement of the Ag atoms compared to the quasicrystal substrate – to be compared with previously published theoretical and experimental findings [5][6][7][8]. There were further sets of data, after thin film growth of four, eight and twenty minutes, used to characterise the type of thin film growth.

2. Theoretical Background

2.1. Quasicrystals

In 1982, Dan Schechtman observed ten-fold symmetry by electron diffraction of a rapidly cooled alloy of aluminium and manganese.[9] It was not until two years later that he published his results for which he won the Nobel prize in chemistry in 2011.[10] In this intervening two years, in an effort to understand the reasoning for the ten-fold symmetry, computer modelling produced this diffraction pattern from an aperiodic 3D structure. It is now accepted that demonstrating a “forbidden” (to periodic crystalline structures) rotational diffraction pattern shows that the material we are working with has an aperiodic structure, and thus is quasicrystalline. An example of an electron diffraction pattern displaying five-fold symmetry is shown in figure 2a, as well as, 2b, a sample of that quasicrystal formed into a shape with five-fold symmetry.

The year after Schectman’s publication, three more quasicrystals were discovered, of eight-fold and twelve-fold rotational symmetry.[11][12] These first quasicrystals were unstable when heated, and it was not until 1987 when many stable quasicrystals were discovered, making further study possible. There are now hundreds of confirmed quasicrystals, of different rotational symmetries and various compositions. In 2009, a naturally occurring quasicrystal was confirmed to exist,[13] and given the name icosahedrite in 2010.[14] The discovery of quasicrystals was a paradigm shift in crystallography, and caused the definition of crystal to be altered and expanded to include the aperiodic nature of quasicrystals.[15]

Quasicrystals have found a range of applications, among them: a coating for non-stick frying pans[2], to reinforce steel for surgical instruments and razor blades, to develop LEDs, diesel engines, insulating materials and new materials that generate electricity from heat[3].

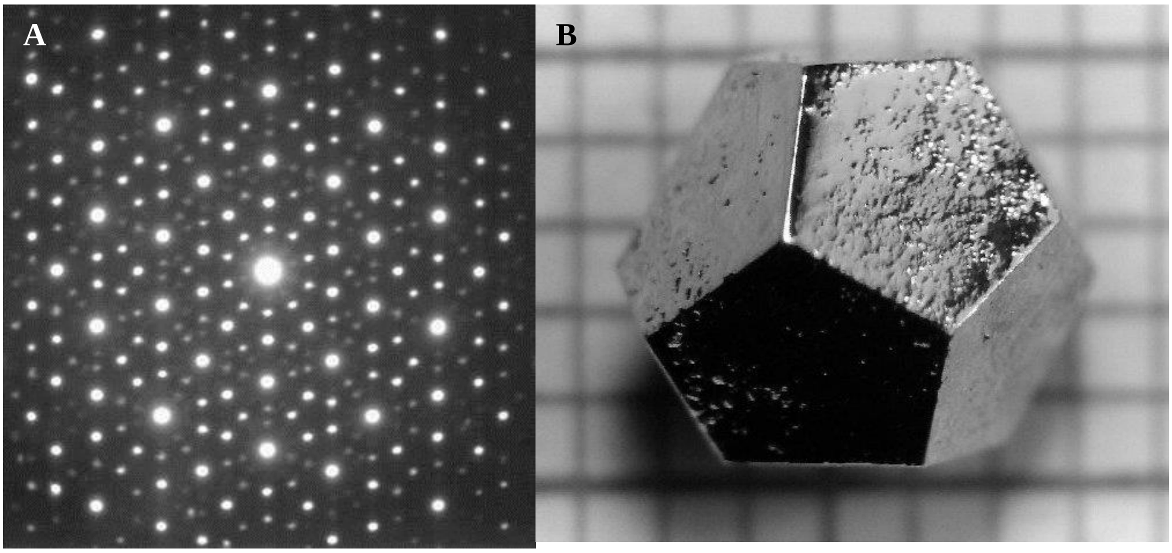

Figure 1:

(a) Electron diffraction pattern of an icosahedral Ho–Mg–Zn quasicrystal
(b) A Ho-Mg-Zn dodecahedral quasicrystal formed as a pentagonal dodecahedron.

2.2. Aperiodic Tiling

Aperiodic tiling's were developed as far back as the fifteenth century, as a decorative element in Islamic architecture (cf. girih tiles)[16]. For study as a field in mathematics, this began in 1961, by logician Hao Weng.[17] Being non-periodic, this means they lack translational symmetry, but have long range order. In the intervening ten years, the number of tiles needed to produce an aperiodic tiling was reduced from a set of 20,426 to a set of six.[18] Work on aperiodic tiling's was furthered by the mathematical physicist Roger Penrose, who was able to reduce the minimum number of tiles to produce an aperiodic tiling to just two.[19] His examples are known as the Penrose tiling's. As Penrose used either pentagons, or shapes related, the Penrose tiling is distinctive by its demonstration of the golden ratio, $\tau = \frac{1+\sqrt{5}}{2} = 1.6180339887 \ldots$[20]

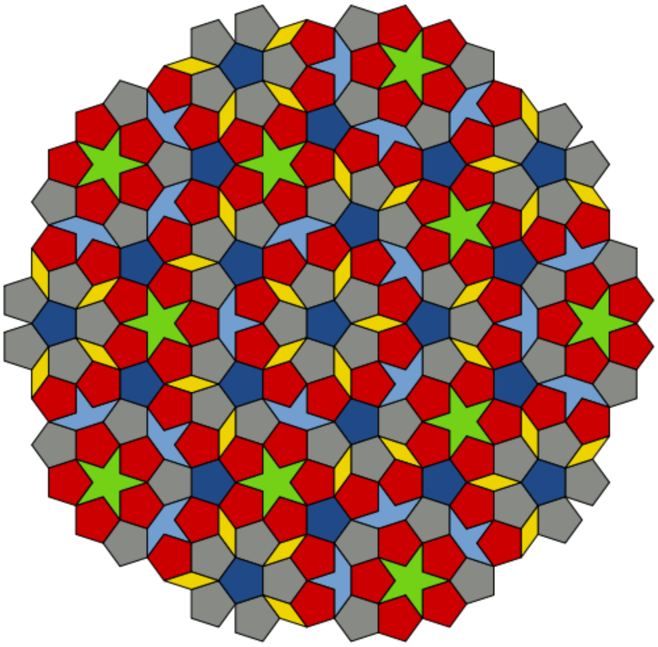

Figure 2: P1 Penrose tiling exhibiting five-fold symmetry. This particular tiling consists of 4 tiling elements: pentagons, pentagrams, diamonds, and a “boat” shape, composed of roughly the upper three-fifths of a pentagram.

The five-fold rotational symmetrical Penrose tiling is of interest in this project, as quasicrystals contain a similar aperiodic order, and as such Penrose tiles can describe the structure of a quasicrystal, and have been instrumental in our understanding of them.[21] Below, in figure 3, a model of the five-fold surface of the i-Ag-In-Yb quasicrystal is shown with P1tiling overlaid. The section I have shown reproduces the pentagons and diamonds, the other tiling elements are not shown by this section. The points of the vertices are at the cluster centres, which will be described in more detail, in section 2.3. The pentagon edge length is 2.5 nm. This model is shown as an outline of what will be recreated on the clean surface of the quasicrystal, in an attempt of reproducing something similar to a previously published paper,[4] shown in figure 4.

Figure 3: A model of the atomic structure on a plane of the five-fold quasicrystal, with diameter 10 nm. The green circles represent Yb atoms, and the purple circles represent Ag and In atoms. The white dots represent the cluster centres. P1 tiling represented by connecting between the cluster centres of Ag and In atoms.

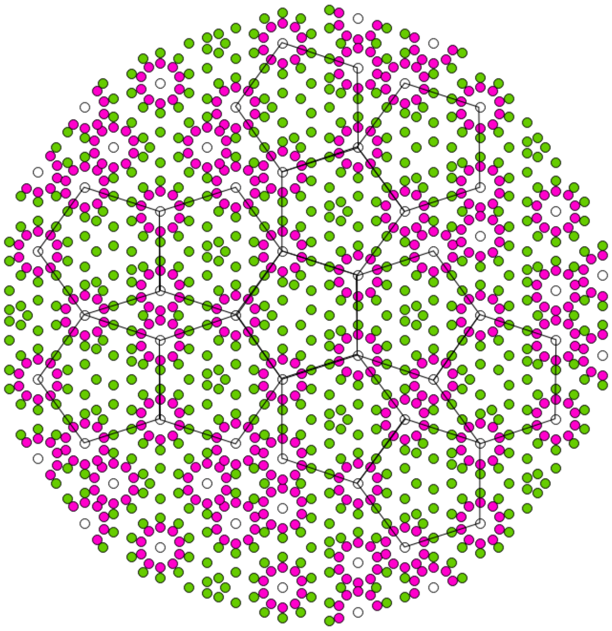

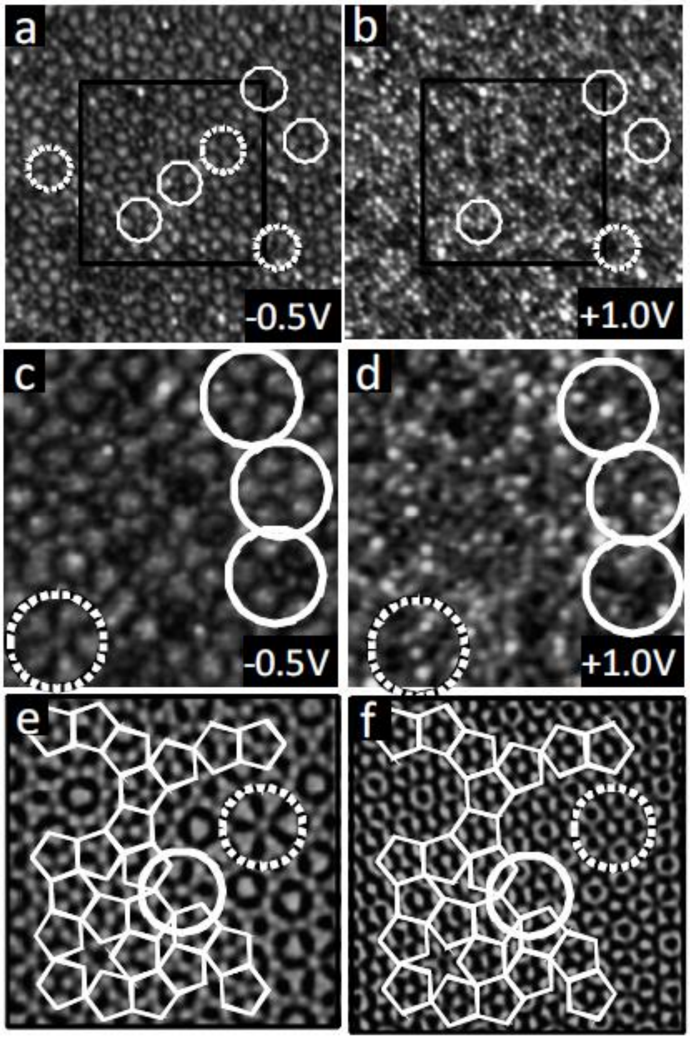

Figure 4: High-resolution STM images of the fivefold *i*-$Ag_{42}In_{42}Yb_{16}$ surface. [(a) and (c)] Images taken at negative bias.
[(b) and (d)] Images taken at positive bias
[(a) and (b): 49 nm x 49 nm; (c) and (d): 23 nm x 23 nm; I_T=1.3 nA, tunneling temperature:
78 K].
The full and dotted circles mark pentagonal features
of two different orientations.
[(e) and (f)] Area marked by a frame in (a) and (b) after Fourier transform pass filtering and with a
pentagonal tiling overlaid.[4]

2.3. Rhombic Triacontahedral (RTH) Clusters

The basic building block of the bulk structure of the *i*-Ag-In-Yb quasicrystal is the rhombic triacontahedral (RTH) cluster.[7] The RTH cluster consists of five successive atomic shells, with few Yb atoms in between, acting as ‘glue atoms’. The RTH cluster is produced in figure 5. The terraces observed on the surface on the quasicrystal are formed at bulk plane intersecting centres of the RTH clusters. It is this plane that is shown above in figure 2, with figure 5b showing a singular cluster centre in gold, which figure 2 shows in white. The cluster centres are within a ring of ten atoms of Ag and In, which corresponds to the cross-section of the fourth shell of the RTH clusters (figure 4a). Each of atoms of the rings of Ag/In is further surrounded by a pentagon of Yb atoms, belonging to either the third shell, or glue atoms.[7] Undergoing STM with a negative bias allows the observation of the Ag/In rings as protrusions. Utilising a positive bias causes the Yb rings to be resolved instead of the protrusions.[4]

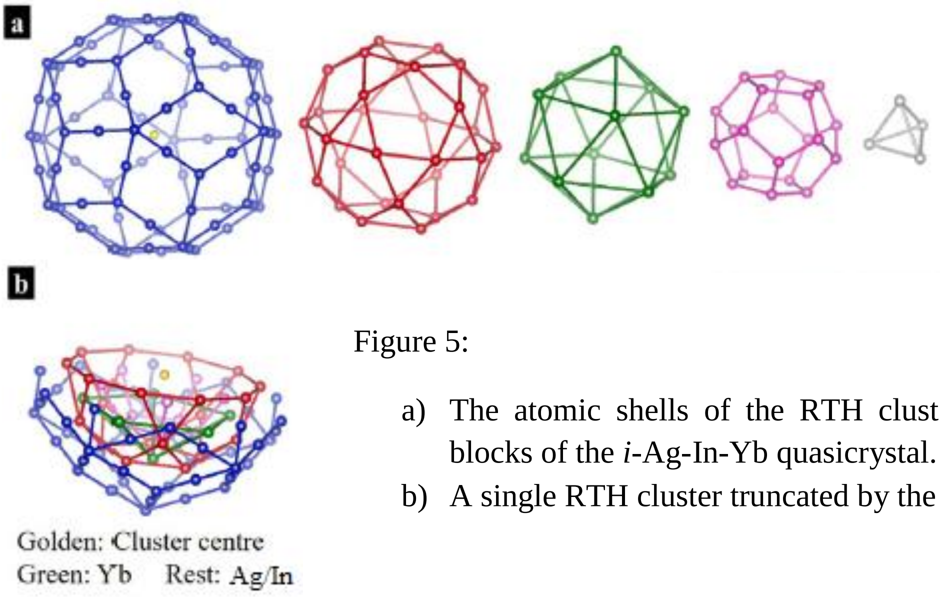

Figure 5:

a) The atomic shells of the RTH cluster, the building blocks of the *i*-Ag-In-Yb quasicrystal.
b) A single RTH cluster truncated by the surface plane.[7]

By looking at the relative position of these cluster centres, the five-fold symmetry can be observed, with each cluster centre being the vertex of a pentagon. It is around these cluster centres that the Ag atoms deposited on the surface are expected to adsorb to.[5] This is demonstrated in figure 6, with the pentagons formed by the Ag atoms drawn on with the dashed line. The adsorption energy is calculated at different heights from the substrate.

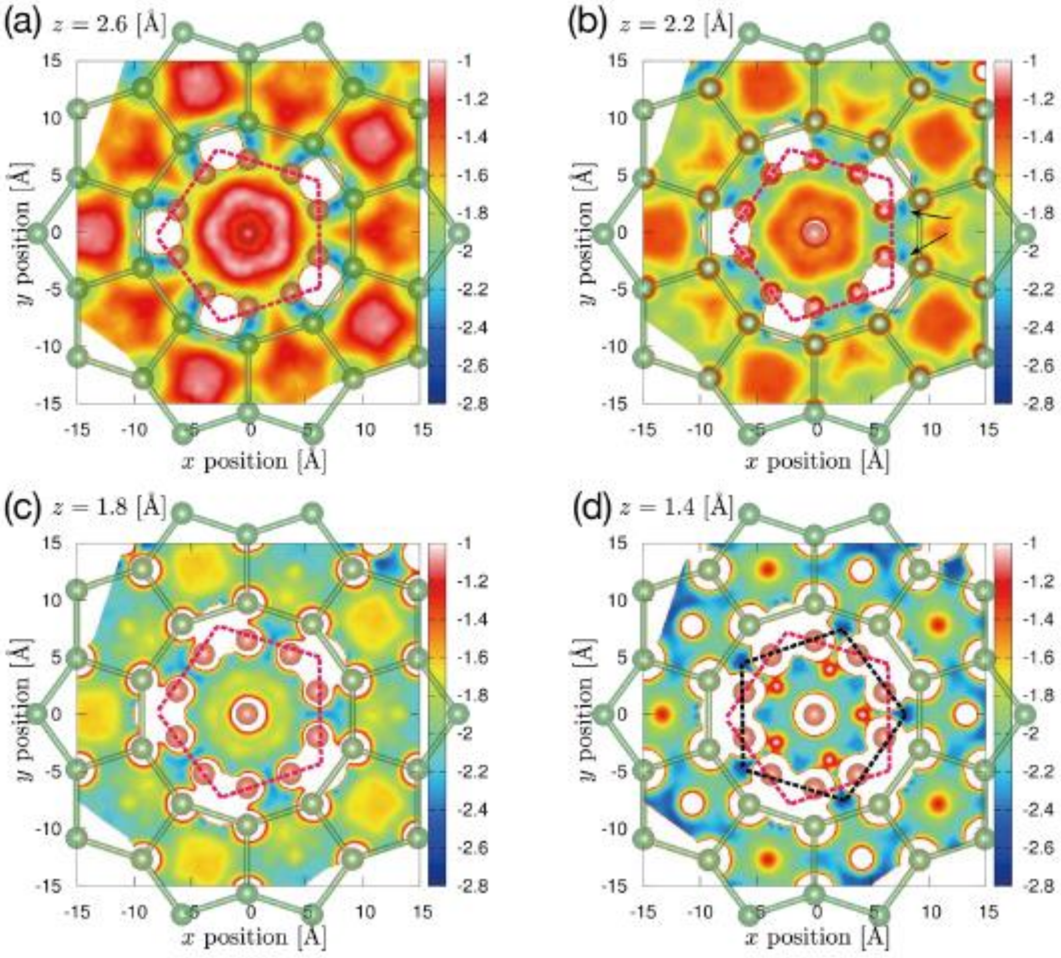

Figure 6: Adsorption energies at each from the surface of the quasicrystal.[5]

2.4. Thin Film Growth

Crystalline growth on a substrate, or epitaxy, is possible if the two materials have a similar lattice constant. A flux of the material to adsorb is produced by evaporation. These atoms, in the vapour phase, are then condensed on the surface of the substrate, in order to cause growth. Growth is not necessarily instantaneous, as atoms may diffuse across the surface until they come across an appropriate place to adsorb, possibly re-evaporate or diffuse into the bulk of the material. Thin film growth experiments often take place under ultra high vacuum conditions to ensure the purity of the films grown.

When a material is deposited on the clean surface of another material, it usually grows by one of three distinct growth modes: Frank-van der Merve, Volmer-Weber or Stranski-Krastanov growth. Frank-van der Merve growth grows layer by layer. A new layer of the adsorbate forms on the previous layer only when the last later has been completed. This is due to the interaction between the substrate and film atoms being stronger than between neighbouring layer atoms. In Volmer-Weber is characterised by the growth of 3D islands of the adsorbate, as new layers start to grow before the previous layer has been completed. This is because of the interactions between the film atoms being higher than that of the film-substrate atoms. Stranski-Krastanov growth is a mix of the previous two growth modes, in that 3D islands are formed after the completion of one or more film layers. This is caused by a certain lattice mismatch between the substrate and adsorbate. As such the film may not continue to produce a thicker film, and so further growth is through the production of the growth of the islands. The three growth modes are summarised below in figure 7.

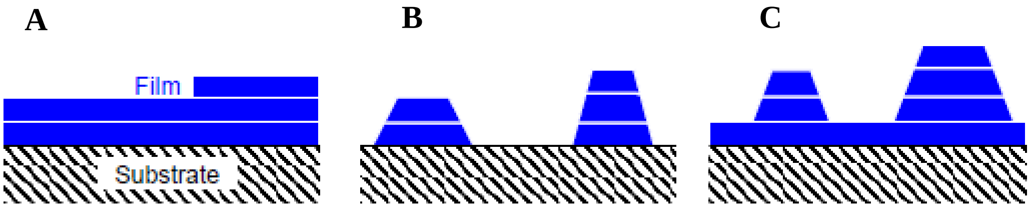

Figure 7: The three most common type of epitaxial growth modes.

a) Frank-van der Merve growth, which grows layer by layer.
b) Volmer-Weber growth, in which islands of the adsorbate grow.
c) Stranski-Krastanov growth, a mixture of the two previous growth modes

3. Experimental Techniques & Data Analysis Tools

3.1. Low Energy Electron Diffraction (LEED)

As mentioned previously, a material can be confirmed to have a quasicrystalline structure if it shows a diffraction pattern that is forbidden to a periodic crystal. As the spacing between the atoms is of the order of 10^{-10} m, this diffraction can be done with electrons. Specifically, low energy electron diffraction (LEED), using electrons with energies of typically 20-500 eV. Via the principle of Bragg diffraction, LEED can give information on the surface morphology and atomic structure, as the electrons can only penetrate a few atomic layers of the surface.

The principle of operation is simple: a collimated beam of electrons are emitted from a hot filament and accelerated to the required energy, being focused onto the sample. The electrons are backscattered and collect on a fluorescent screen, with a high positive voltage to accelerate the electrons to sufficient kinetic energy in order to cause light emission. Electrons not elastically scattered are filtered out by applying voltage to grids before the fluorescent screen. These grids ensure that only elastically scattered electrons contribute to the diffraction pattern. A characteristic diffraction pattern for the material in then produced, consisting of bright spots, which are then recorded on a camera. A diagram of the apparatus of LEED is shown in figure 8.

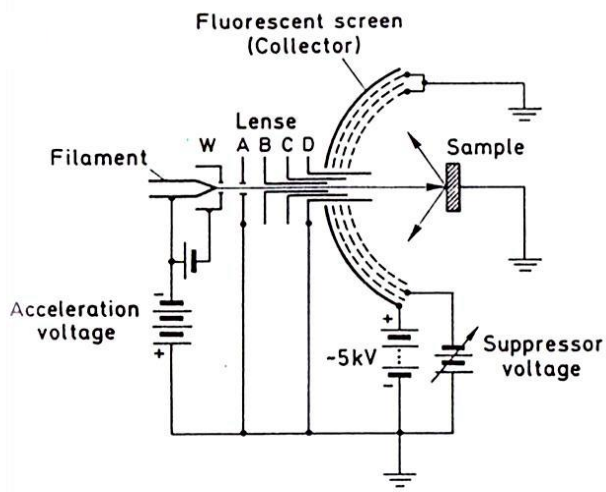

Figure 8: Diagram of LEED optics apparatus.

3.2. Scanning Tunnelling Microscopy (STM)

The scanning tunnelling microscope was invented in 1981, winning its inventor the Nobel Prize in physics in1986.[22] Using an atomically thin metallic probe and bringing this extremely close to the sample being scanned (<1 nm), a voltage is applied, and due to the quantum mechanical tunnelling effect, a current will be detected as electrons tunnel from the sample to the probe tip (and vice versa, depending on the voltage bias). With the sample at positive bias, the unoccupied states of the sample are probed – at a negative sample bias; the occupied states of the sample are probed. This current is proportional to the local density of states at the Fermi level. The sharp metallic tip of the probe is usually made of tungsten, although platinum-iridium and gold tips are also used.[23] A tungsten tip was used in this project. STM can produce 3D images of the surface of conducting solids with lateral resolution of 0.1 nm and depth resolution of 0.01 nm. With resolution of this precision, individual atoms that form the sample can be imaged. Figure 9 shows a schematic view of an STM.

The tunnelling current, which produces the image, is extremely sensitive to the separation of the probe tip and sample, due to the exponential nature of quantum mechanical tunnelling, which gives a high resolution perpendicular to the surface. The lateral resolution is dependent on the tip shape, needing to be atomically sharp to provide the highest resolutions.

Two modes can be employed when using STM, constant height or constant current mode. In constant height mode, the z-direction is fixed while the tip scans in the xy-plane, however this is unsuitable for rough surfaces due to potential tip collisions with surface protrusions. Constant current mode is more commonly used, wherein the distance between the tip and surface is fixed, and hence the tunnelling current is also fixed, by allowing movement in the z-direction. Constant current mode allows rough images to be imaged, but this is slower compared to constant height mode due to the need to keep the probe at a constant height relative to the surface to retain to the same current flow. Constant current mode was used in this project.

Applications of STM include nano-engineering by atomic manipulation, understanding the surface atomic structure, magnetic properties of a surface, and the electronic properties of the surface.

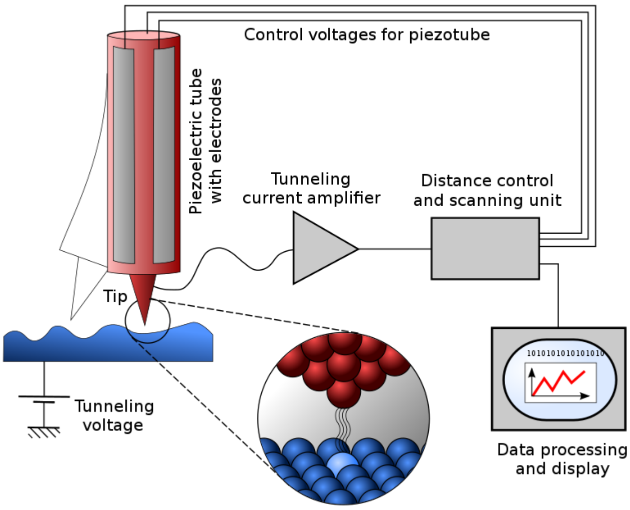

Figure 9: Schematic view of an STM

3.3. Ultra High Vacuum (UHV) Technology

Both the LEED and STM parts of this project where undertaken in ultra high vacuum environments. Ultra high vacuum environments are a necessity for most surface science experiments in order to minimise and avoid both the interference of the probe and detected particles with atmospheric gas particles, and contamination of the surface in order to maintain a clean surface for the duration of the experiment. Ultra high vacuum is a pressure of the order 10^{-10} Torr, which gives a mean free path much larger than the dimensions of the experimental chamber, ensuring the surface will remain clean.

Ultra high vacuum chambers are typically made of stainless steel, which has a low outgassing rate. A high vacuum is obtained using different vacuum pumps, which is measured with pressure gauges. The chamber is constructed to be “baked” at 470 K while the pumps operate, this accelerates the desorption of water vapour and other gases from the internal surfaces of the chamber.

In a UHV chamber, the pressure is measured by an ionisation gauge. Electrons are thermally emitted from the cathode and accelerated by the anode potential; this causes the ionisation of gas molecules as they move towards the anode. The current produced by the ions is related to the ambient pressure in the chamber. The residual gas in the chamber can by analysed via mass spectrometry.

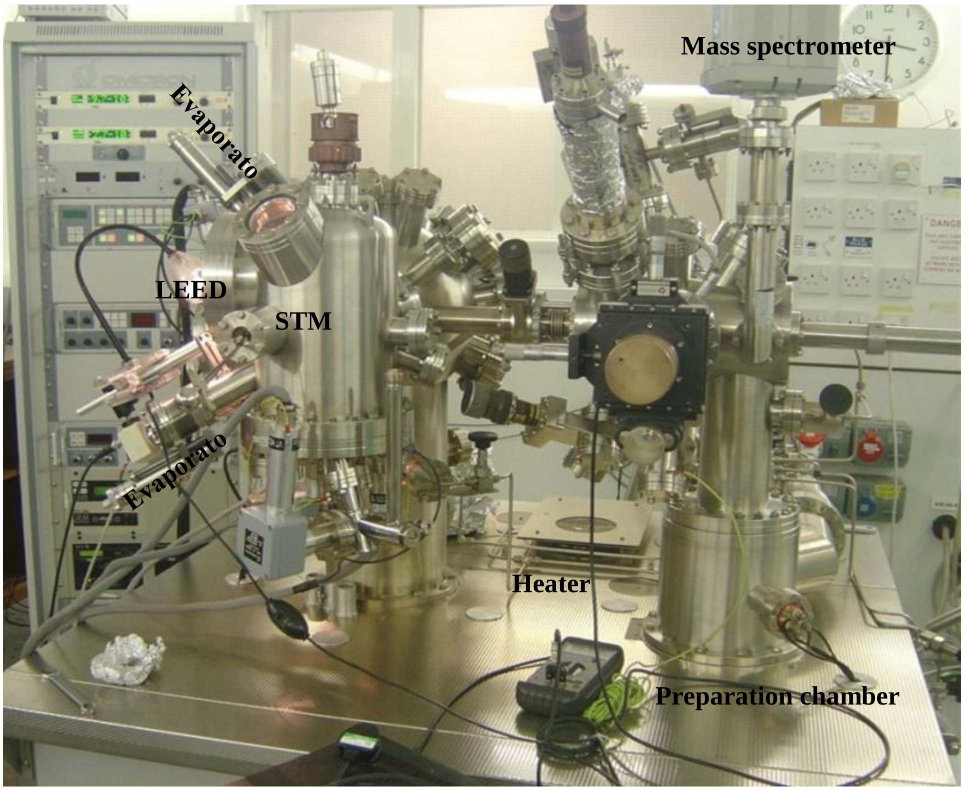

Figure 10: UHV chamber equipped with STM and LEED.

3.4. WSxM

WSxM[24] is an application for data acquisition and processing in scanning probe microscopy. The majority of data analysis for this project was by using this programme. The analysis of the step heights was done using the profile tool, an example of which is shown in figure 11. The profile tool allows a line to be drawn between any points, which produces a graph of the distance moved along the line against the vertical height. This graph can then be further analysed, selecting points on the graph to compare, which would give a value for the vertical height between steps utilised to find the step heights.

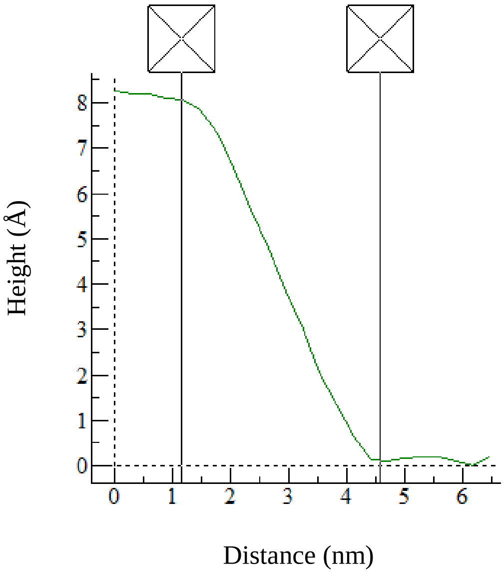

Figure 11: Example image of the graph produced by using the profile tool across a step in WSxM, including further measuring points on the line. The vertical height measured between the two lines was given as 8.2 Å.

In order to produce the Penrose tiling, it was first necessary to produce an image of a zoomed section of the surface filtered through a fast Fourier transform – this allows easier viewing of the underlying pattern on an atomic level. A fast Fourier transform is the conversion of a signal from its original domain into a representation in the frequency domain,[25] in this example from real space into reciprocal space. The filtered images can then be drawn over, recreating the pentagonal, five-fold symmetry. This was done for the same section on two images, one at positive bias, and the other at negative bias.

In regards to analysing the STM images during the thin film growth of silver atoms, for the data considered low coverage: the main analysis was done by producing videos of consecutive images. These videos were then further analysed, paying attention to the movement of the silver atoms, the pentagonal vertices that they stop on, in order that these may be measured. The measured pentagon side lengths were then compared with theoretical values from a previous paper on the growth of a thin film of silver atoms on this quasicrystal. This was also done similarly for the higher coverage data.

3.5. IGOR Pro

IGOR Pro is a multipurpose scientific data analysis software, utilisable for graphing, curve fitting, presentation, analysis and statistics, communication, image analysis, data formatting, data acquisition and programmability.[26] For use in this project, a file was given of a model of the structure of the icosahedral cadmium-ytterbium quasicrystal, as the structure of the Ag-In-Yb quasicrystal being considered in my project has exactly the same structure, albeit with equal proportions of silver and indium atoms replacing the cadmium atoms in the model. The image in figure 2 is from IGOR Pro. IGOR Pro was used to find the model heights between potential surface planes as well as the plane structure at the five-fold surface

4. Data Analysis & Results

4.1. LEED

Figure 13 shows the results of LEED, wherein a sample of the *i*-Ag-In-Yb quasicrystal was bombarded by a beam of electrons. The bright spots caused by the electrons diffracting due the Bragg condition can clearly be shown, and the resulting pattern shows five and ten-fold rotational symmetry, indicative of quasicrystalline structure and a well prepared flat surface needed for further deposition experiments. The distance between the first and second order diffraction is shows τ-scaling, which is also indicative of quasicrystalline structure, however that was not calculated here, as it was easier to do so using the STM data in section 4.2.2.

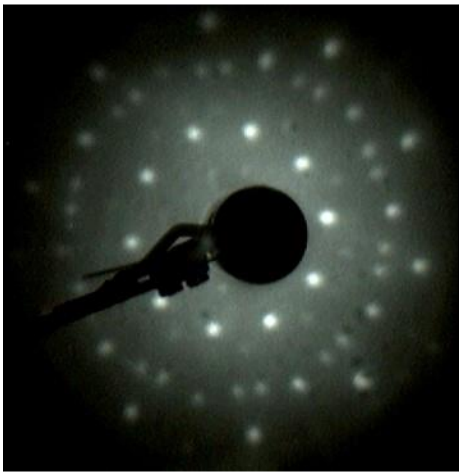

Figure 13: LEED result from an *i*-Ag-In-Yb quasicrystal.

4.2. STM

4.2.1. Step Height

Considering the clean surface of the quasicrystal, one day's worth of STM data was analysed, compromising nine images with various terraces on. Every single step was measured by height and put in a table, totalling 69 steps. The previous paper on the characterisation of this quasicrystal,[2] explains that there are three different step heights, labelled S, M and L, with S = 0.28(±0.04) nm, M = 0.58(±0.03) nm, and L = 0.85(±0.05) nm. The values of the steps obtained were then collated into three groups, around each height for S, M and L, for comparison purposes. A theoretical value of each of the step heights were found using the model on IGOR Pro, which were found to be S = 0.2544 nm, M = 0.5689 nm, and L = 0.8234 nm. The data that the step heights were calculated from is shown in figure 14.

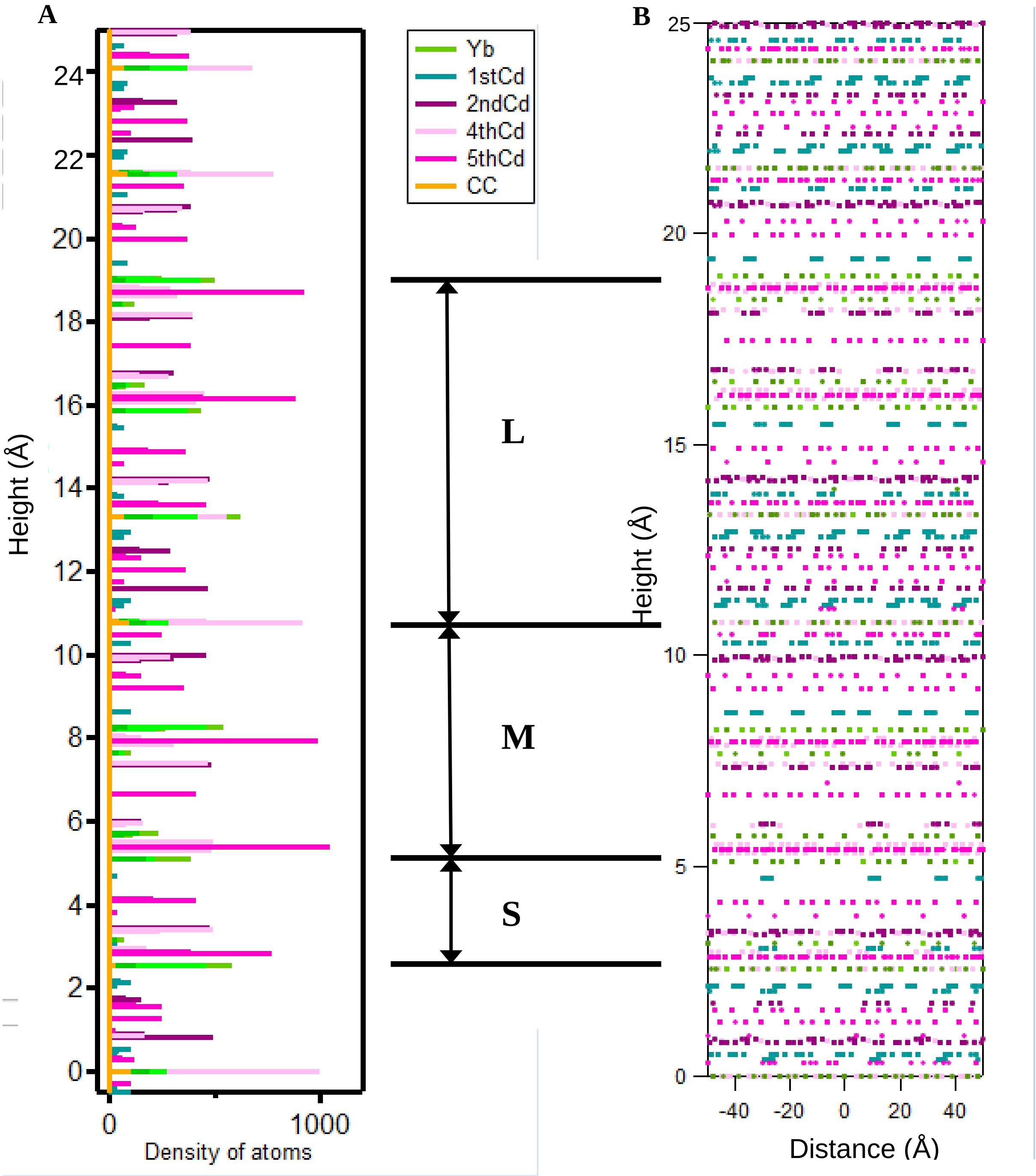

Figure 14: Data from IGOR Pro, showing one example of each of the three step heights. Note: as mentioned in section 3.5, the model given was for the *i*-Cd-Yb quasicrystal, as this is identical in structure to the *i*-Ag-In-Yb quasicrystal, with the Cd atoms being replaced by equal amounts of Ag and In atoms.

Once the data was collated, the average for each of the three step heights was calculated, as well as their standard deviation and standard error. Below this are the values and error for the three step heights from the previous paper mentioned, as well as the values given in the model. Finally, a consistency check to 3σ is done for each of the comparative values with this data, being consistent if the top line of this (|A-B|) is a smaller value than the bottom line ($3(a^2+b^2)^{0.5}$).

	S	**M**	**L**
total	31	19	19
avg height (Å)	2.6	5.6	8.5
sd (Å)	0.28	0.45	0.81
error (Å)	0.051	0.1	0.0023
Previous paper: given value (Å)	2.8	5.8	8.5
error (Å)	0.4	0.3	0.5
Model: given value (Å)	2.5	5.7	8.2
Paper: $\lvert A-B \rvert$	0.2	0.2	0
$3(a^2+b^2)^{0.5}$	1.2	0.95	1.5
	consistent	**consistent**	**consistent**
Model: $\lvert A-B \rvert$	0.1	0.1	0.3
$3(a^2+b^2)^{0.5}$	0.15	0.3	0.0069
	consistent	**consistent**	inconsistent

Table 1: Table containing data from measuring the step heights of nine STM images in WSxM, each collated around one of three step heights in a previous paper, labelled S, M and L. The average value (avg) for these is given, as well as standard deviation (sd), and standard error (error).

Reconsidering the nineteen points collated for step L, as consistency was not achieved between this data and the model, they range from 7.84 Å to 10.56 Å, however only three data points are larger than 9 Å (9.97 Å, 10.12 Å and 10.56 Å, respectively). Discounting these three noticeably larger data points, and recalculating gave a new value for L of 8.2(85) Å, the same as the theoretically derived value to 2 significant figures. This new value of L was found to be consistent with both the theoretical value and the previously published value.

4.2.2. Atomic Structure

As mentioned above, in section 2a, the icosahedral Ag-In-Yb quasicrystal has a characteristic five-fold symmetry. Figure 2, of the same section, shows a model of the five-fold structure of the atomic surface, taking a section of this and connecting between the Ag and In clusters demonstrates the symmetry.

Using the process described in section 2d, which is shown in figure 15, this produced the filtered images displayed in figures 16a and 16c. A section of Penrose tiling has been overlaid on both. Figures 16a and 16b were produced using a negative bias, figures 16c and 16d were produced using a positive bias. At negative bias, which shows the occupied states, the vertices of each tile lie at the protrusions observed by STM. At positive bias, which shows the unoccupied states, the vertices reside at the centre of rings observed by STM. This is consistent with the previously published data.[4]

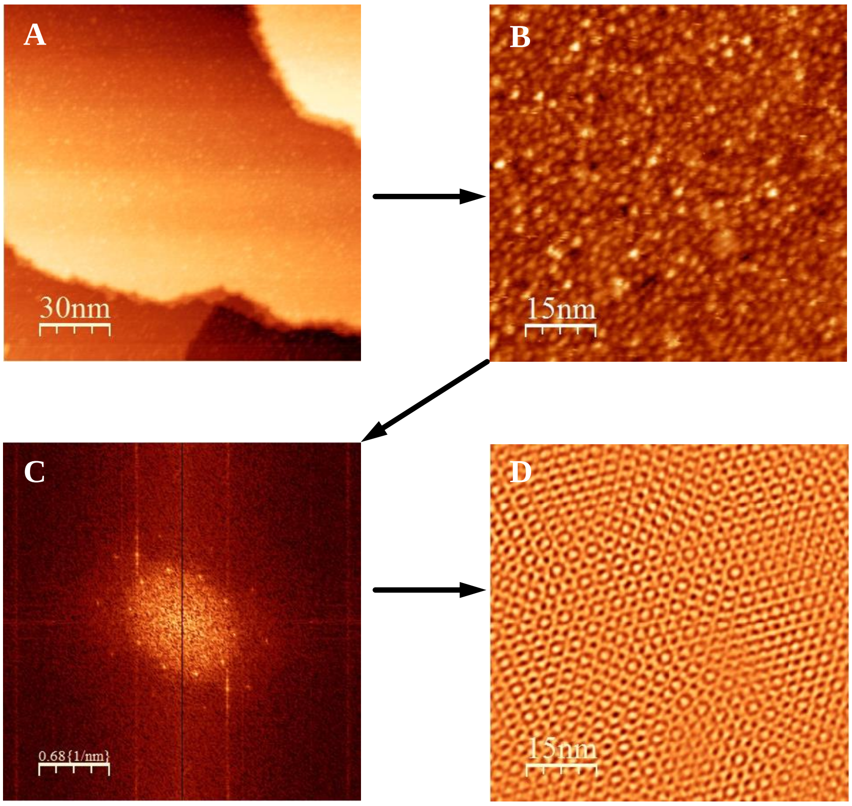

Figure 15: Abridged process of producing a Fourier transform filtered image in WSxM, using an image at negative bias.

(a) Original image
(b) Image after both zooming in and then flattening.
(c) Image (b) through a fast Fourier transform.
(d) Filtered image produce by highlighting the first order diffraction spots (the 10 bright spots around the large central bright spot), as well as the second order bright spots. This is the image used to recreate the Penrose tiling.

Although the filtered image produced was as large as possible (73 nm x 73 nm), it was easier to overlay the Penrose tiling over a smaller section of this. The same section was used for both the negative and positive bias for comparison, a 20 nm x 20 nm section of the upper right corner of figure 15d. Figure 17 shows the comparison between the modelled view of the pentagon tiles, next to an actual pentagon observed at negative bias (17b), and another at positive bias (17c).

Figure 16: Four images showing the fivefold symmetrical nature of the Ag-In-Yb quasicrystal via Penrose tiling:

a) A section from the upper right corner of figure 15d, overlaid with pentagons.
b) The same image as (a), before it was filtered through a fast Fourier transform.
c) The same section as (a), however this time with a positive bias.
d) The same image as (c), before it was filtered through a fast Fourier transform.

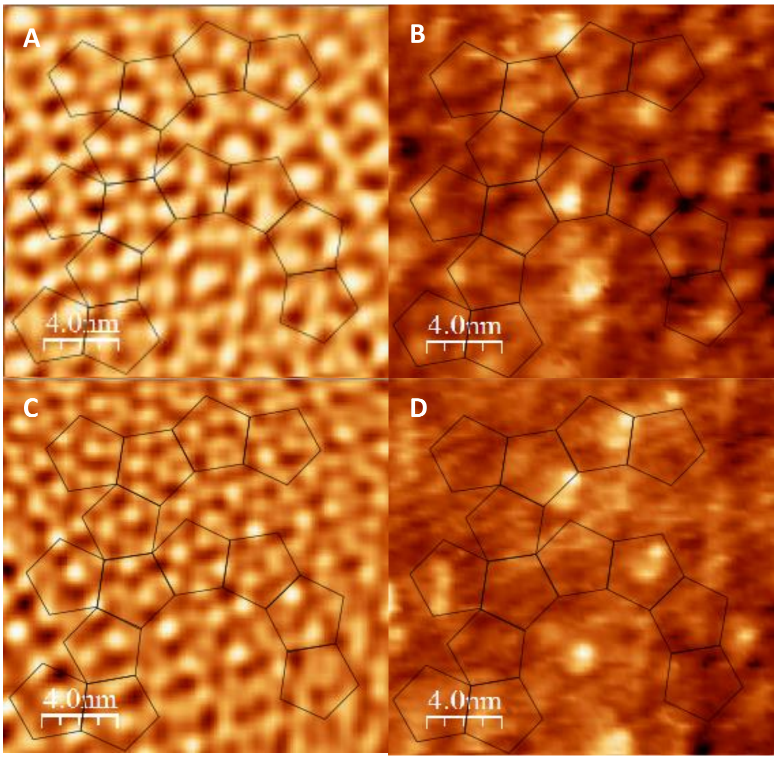

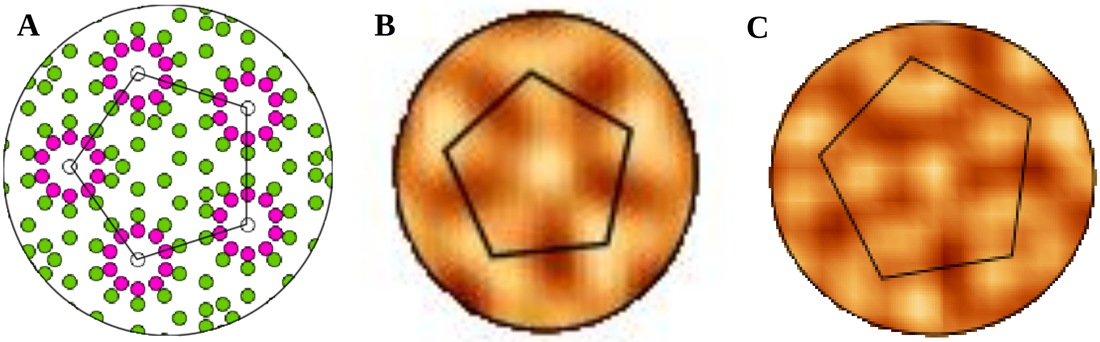

Figure 17: Comparison of (a) the model structure of the pentagons formed between the cluster centres, with data collected at (b) negative bias, and (c) positive bias.

Using figure 15c, a FFT at negative bias, the tau-scaling can be observed. This was done by measuring each of the five opposite pairs of both first order and second order bright spots (the ten bright spots around the edge of the central ring, and the further ten beyond those). The average length of the first order bright spots was 0.99 nm^{-1}, and the average length of the second order bright spots was 1.61 nm^{-1}. Dividing the second length by the first gave a ratio of 1.62, this is $\tau = \frac{1+\sqrt{5}}{2}$ to 3 s.f. A further check ensured the consistency between the given value of τ and what was calculated.

4.2.3. Thin Film Growth

In regards to the deposition of Ag atoms on the surface of the Ag-In-Yb quasicrystal, several times to deposit the Ag atoms were trialled. The initial set of data was for 45 seconds. STM data for other times was also produced, including four minutes, eight minutes and twenty minutes. All these were done at room temperature.

Figure 18 shows six consecutive images of a close up of one prominent pentagonal feature of the quasicrystal substrate, circled in red in 18a. This would make up one of the vertices of the pentagons drawn in the previous section, being a cluster centre. This STM data was taken after 45 seconds of Ag deposition, with a -0.6 V bias. As can be seen in figure 18b and 18d, and 18c, there are two points that the silver atoms adsorb to that would form the vertices of a pentagon. These silver atoms are circled in red through 18b-18d. That the Ag atoms adsorb here is expected from the previously published theoretical paper.[5] This paper tells us that the side length of the pentagons formed by the Ag atoms would be 1 nm. Pentagons were drawn on each section of figure 18 containing an Ag atom, as is shown, in order to calculate an average side length of the pentagons that would be formed by the adsorption of the silver atoms. This was calculated to be 1.06±0.05 nm. Of all the data, this shows the clearest example of the silver atoms diffusing across the surface of the substrate protrusions. Two further examples of surface diffusion have been highlighted on figure 18, within the white circled areas. The Ag atoms are not adsorbing as strongly to the expected sites as theorised, hence the surface diffusion.

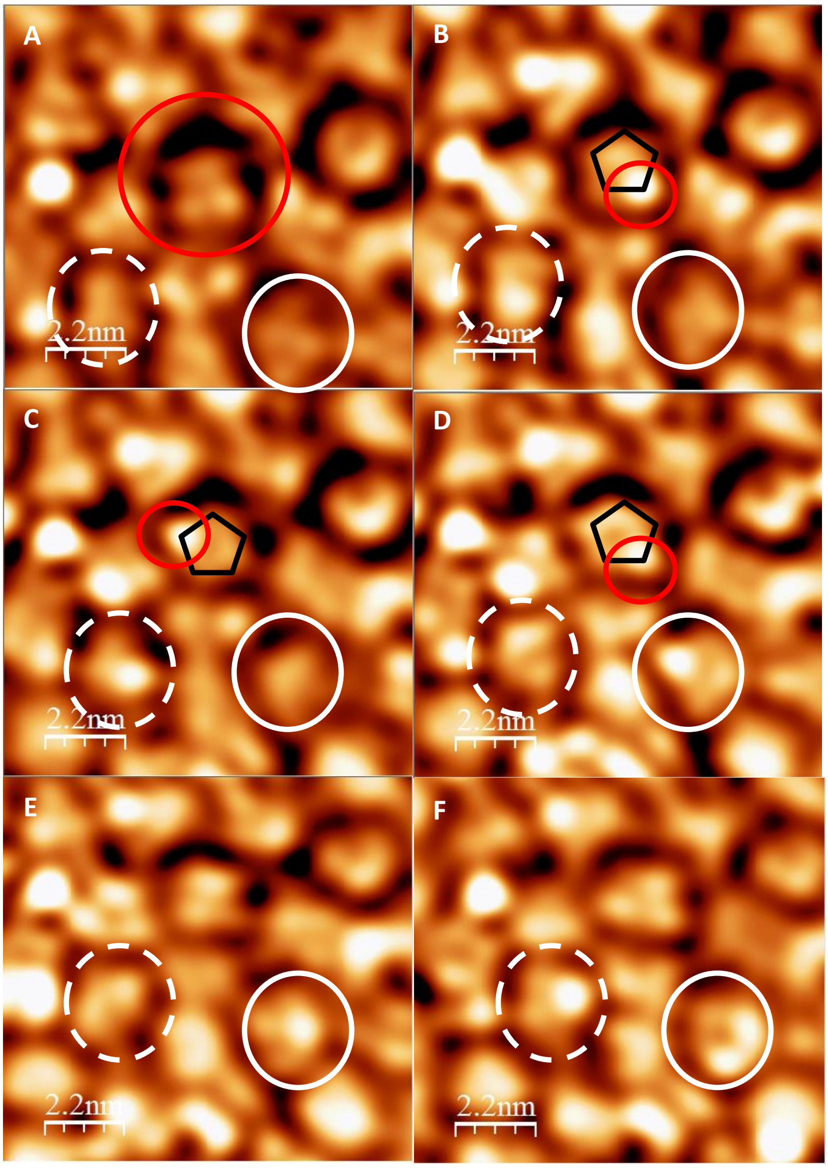

Figure 18: Consecutive images focusing on a pentagonal feature of the quasicrystal substrate after 45 seconds Ag deposition.

The next sets of data to be analysed were after deposition of silver for four minutes, eight minutes, and finally twenty minutes. Figure 19 shows consecutive images of a 20 nm x 20 nm of the surface of the quasicrystal after four minutes of silver deposition. The white circles highlighting the same section across the consecutive images, providing evidence of continuing surface diffusion. The bright spot of a silver atom can be seen to appear and disappear across the four images in the dashed circle, as well as the solid circle which contains a silver atom for 19b and 19c, before vanishing in 19d. What is much more noticeable on this data, however, are the large brighter features beginning to form – the development of thin film growth. It is too early in the process to distinguish the type of growth.

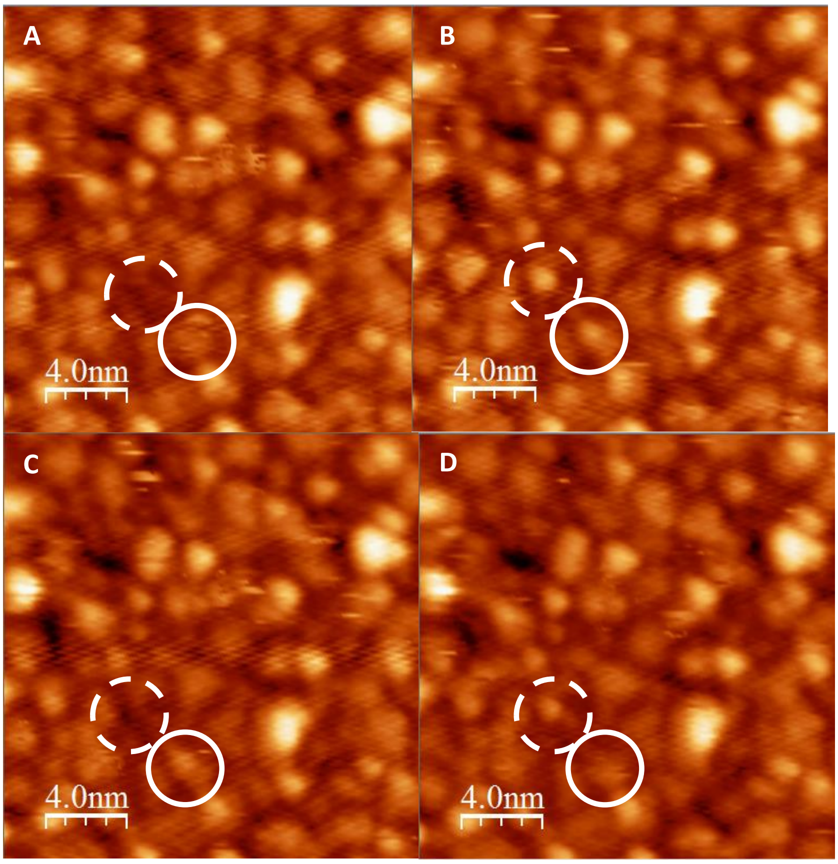

Figure 19: Consecutive images of STM after four minutes of silver deposition. The brighter features are the development of thin film growth.

Figure 20 takes the same size section of the surface as figure 19, for consecutive frames, however this time after eight minutes of silver deposition. Comparatively, it can be seen that the islands are becoming larger, and also more defined compared to the four minute deposition data. Larger sections of the adsorbate are connected together, perhaps indicative of the silver wetting the surface densely, as is found in the growth of a thin film of lead on this quasicrystal.[8].Surface diffusion still takes place, highlighted similarly to figure 19. Figure 21 was produced by the 20 minute silver deposition data, similarly to the previous figures. This also still shows some surface diffusion. Also included (figure 21f), is one of the images that was zoomed in to produce one of the other images. This shows a larger area (120 nm x 120 nm), showing more clearly how the thin film growth has developed, there appears to be a layer forming as there are many parts connecting, however with some islands beginning to form on top of this. This is indicative of Volmer-Weber thin film growth.

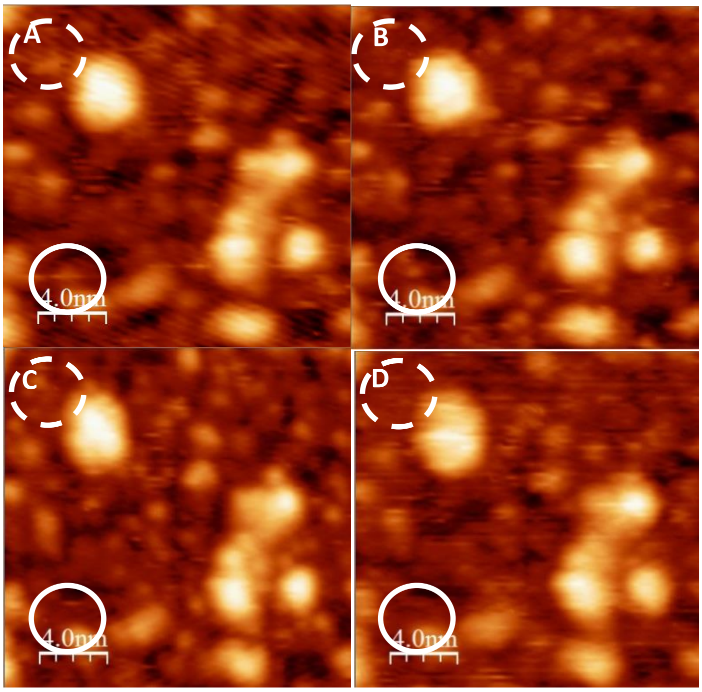

Figure 20: Consecutive images of STM after eight minutes of silver deposition.

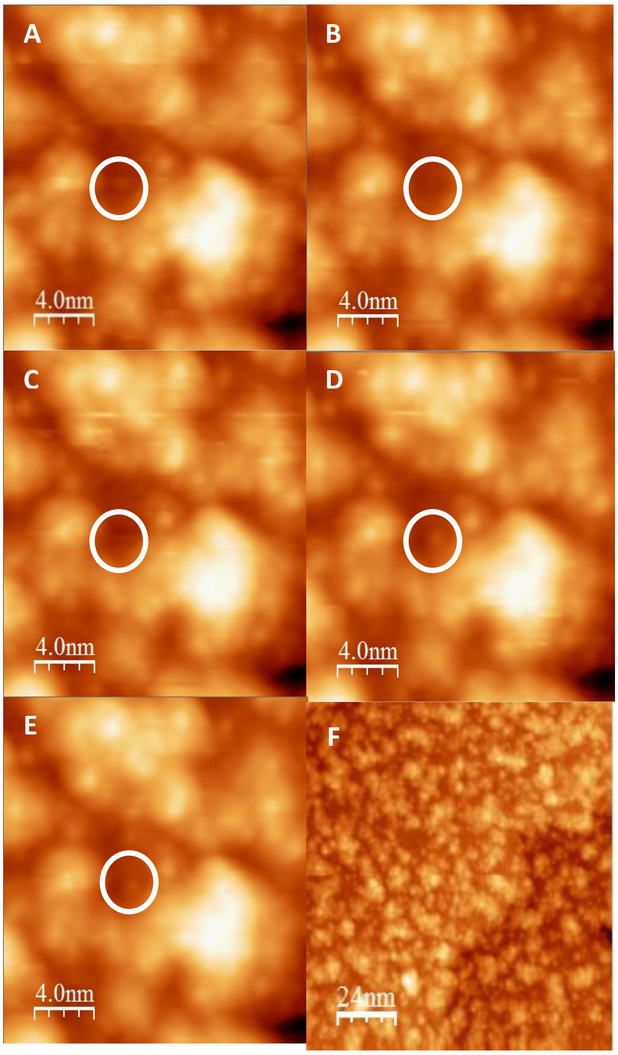

Figure 21: Consecutive images of a 20 nm x 20 nm of STM data after 20 minutes of silver deposition. Surface diffusion is still observable, as encircled like the previous examples. In this 20 nm x 20 nm section, there is almost a complete layer grown of silver.

5. Discussion & Conclusion

In regards to characterising the clean surface of the quasicrystal, this can be compared to both theoretical data and previously published experimental data. Table 1, in section 4.2.1, has this tabulated for the step height data that was measured from the clean surface STM data. For the average value of each of the three step heights, consistency was achieved between what was calculated and both the theoretically derived values and previous experimental results. The three values for the L step height that were disregarded in the recalculation, as mentioned in section 4.2.1, could have possibly been due to the bunching of an L and S step, or two M steps. (The corrected version, table 1a, with the larger values for L discounted can be found in the appendix below, section 7a).

The five-fold Penrose tiling used to show the structure of this quasicrystal is known as P1[27]. This consists of four tiling elements, a pentagon, a pentagram, a diamond and a shape roughly the top three-fifths of a pentagram. From my tiling over the model in figure 16, this clearly shows connected pentagons, and there are two examples of the diamond shape formed.

As for my attempt at recreating the Penrose tiling over the STM data in figure 16, it is clear that there is a five-fold rotational symmetry due to the interconnected pentagons, however utilising the small section that was tiled did not produce any of the other three tiling elements. Although, it can be seen on the left hand side that there appear to be two stars forming, that could have possibly been filled out if there was more of the image to the left. In the top central section there is almost a diamond formed too, lacking one side. Although tiled incompletely, and for a small section, with the partial appearance of the majority of the P1 tiles, this is enough to confidently say that this tiling characterises the surface of the quasicrystal, showing its five-fold nature. This points towards a well-prepared, atomically clean surface with the expected atomic structure, as is necessary for deposition experiments. This is also observable through the symmetry given by the FFT images produced, one such example already shown is figure 15c in section 4.2.2. The five-fold nature was also confirmed by the τ-scaling between the first and second order points of the FFT/ The ratio between the was calculated as 1.62, τ to 3 s.f., and consistency was achieved between this calculated value and τ.

The final version of the tiling was the fifth attempt, after a couple of false starts, as well as failing to tile the same section to both positive and negative biases initially. There was a lot of trouble with this section, initially due to trying to tile a relatively large image, 73 nm x 73 nm, from which there were only three sections producible of relatively few and disjointed pentagons. After tiling the model, which shows only 10 nm x 10 nm, a smaller section was then considered to tile, zooming in to a 20 nm x 20 nm section. This made it much easier, allowing to tile much clearer. The main problem with tiling was selecting a pentagon tile size, that when copied would exactly represent the structure beneath it, while still connecting to the previous pentagon, as deciding the change the size of pentagons used requires a complete retiling and seeing if that lines up better with the underlying image. Initial attempts drifted quickly, to the point where few of the drawn pentagons drawn would line up to the pentagonal shapes beneath. By making the section considered much smaller, comparable to the size of the model, this made it easier to draw on, although some drift can still be seen: the first pentagons where on the left hand side of the image and the further rightward pentagons are less lined up. Attaining a perfect tiling would be just a matter of practice and time, however, after having already spent the most time on this section of the analysis in comparison to any other part of the project, I believe the current attempt reasonably shows the five-fold rotational symmetry via Penrose tiling, although this would be the first thing to be improved on in any further work.

The Penrose tiling could have been improved by making a drift correction, manipulating the fast Fourier Transform to produce a more symmetrical, circular pattern. This was undertaken, but there was great difficulty with trying to line up both images, and their tiling's, and so it was left out, with the earlier attempt kept in this report.

This is essentially the completion of the preliminary section of the report, that being the characterisation of the clean surface of the quasicrystal, with reference to theoretical models and previous published results. The next section will consider the thin film growth of silver on the surface of the quasicrystal.

The previous published theoretical paper on silver adsorption by this quasicrystal[5] suggests that the silver atoms will form pentagons on the vertices of the pentagonal Penrose tiling. These pentagons will have a side length of approximately 1 nm. From my 45 second silver deposition analysis, I calculated the pentagons formed by the silver atoms to be of side length 1.06±0.05 nm. A 3σ consistency check makes my value consistent with the theoretical value. This means that the silver atoms are adsorbing at the sites that we expect, although not adsorbing as strongly as we would expect, this is apparent due to the large amount of surface diffusion visible. A previous paper regarding the growth of a thin film of bismuth on the same five-fold surface of the quasicrystal[7], these were also formed into pentagons, with edge length of 0.95±0.05 nm, shown in figure 22. Comparing the pentagon side length of bismuth with the side length of the pentagons that were observed with silver, these are of consistent length to within 3σ.

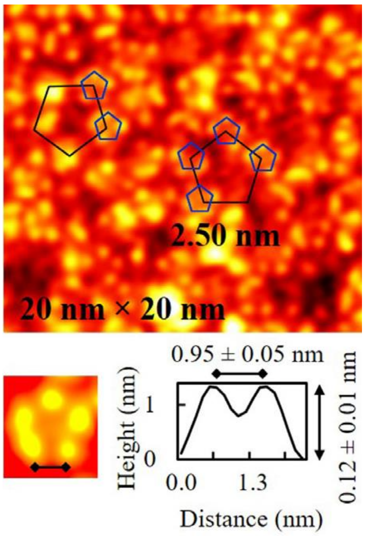

Figure 22: Pentagon side length for Bi adsorbed on the surface of the *i*-Ag-In-Yb quasicrystal.[7]

Throughout the entirety of the STM data, surface diffusion is visible, as mentioned previously, this suggests that the silver atoms do not adsorb as strongly as expected. With the higher coverage silver deposition data, it is hard to tell whether any of the islands of silver atoms display any internal structure. As such, we cannot say whether they crystalline or quasicrystalline. This is unlike the case of Bi, which clearly formed crystalline islands, unlike Ag here. Considering the data after 20 minutes of silver deposition, the thin film growth of silver on this quasicrystal can be characterised as Volmer-Weber growth, with the thin film having the natural structure of crystalline Ag.

Concluding, the clean surface of the *i*-Ag-In-Yb quasicrystal was successfully characterised, with consistent step heights found in comparison to theoretical modelling and previously published results, as well as P1 type Penrose tiling demonstrated, and τ-scaling demonstrated. As for the characterisation of a thin film of silver of the surface, the type of growth was characterised, yet the internal structure of the growth was not. This shows one way in which further work on this topic can be carried out, as well as considering utilising higher temperatures during the silver deposition, as all the data obtained for this project was collected only at room temperature.

[Word count: 6,339]

6. References

1. D. Shechtman, et al., "Metallic Phase with Long-Range Orientational Order and No Translational Symmetry" Physical Review Letters 53 (20): 1951–1953 (1984)
2. J. Fikar, “Al-Cu-Fe quasicrystalline coatings and composites studied by mechanical spectroscopy,” École polytechnique fédérale de Lausanne EPFL, Thesis no. 2707 (2002)
3. M. Kalman, “The Quasicrystal Laureate,” MIT Technology Review (October 2011) available from: https://www.technologyreview.com/s/425729/the-quasicrystal-laureate/
4. H.R. Sharma, et al., “Structure of the fivefold surface of the Ag-In-Yb icosahedral quasicrystal” Physical Review B 80, 121401(R) (2009)
5. K. Nozawa, “Fist-Principles Study of Adsorption of Ag on Ag-In-Yb Quasicrystal Surface” ISCEAS-0158
6. H. Sharma, et al., “Templated Three-Dimensional Growth of Quasicrystalline Lead,” Nature Communications 4:2715 (Nov 2013)
7. S. S. Hars, et al., “Growth of a Bismuth Thin Film on the Five-Fold Surface of the Icosahedral Ag-In-Yb Quasicrystal,” Surface Science 678 (2018)
8. S. Coates, et al., “Influence of Orientational Bulk Density on the Growth of Pb on the i-Ag-In-Yb Quasicrystal,” yet to be published, (2020)
9. “Quasicrystal Discovery” (October 2011) available from: https://web.archive.org/web/20111007225727/http://www.quasi.iastate.edu/discovery.html
10. J. Carpenter, “Nobel win for crystal discovery,” BBC News, (October 2011) available from: https://www.bbc.co.uk/news/science-environment-15181187
11. T. Ishimasa, H.-U. Nissen, Y. Fukano, "New ordered state between crystalline and amorphous in Ni-Cr particles," Physical Review Letters. 55 (5): 511–513 (1985)
12. N. Wang, H. Chen, K. Kuo, "Two-dimensional quasicrystal with eightfold rotational symmetry," Physical Review Letters. 59 (9): 1010–1013 (1987)
13. L. Bindi, P.J. Steinhardt, N. Yao, P.J. Lu, "Natural Quasicrystals," Science 324 (5932): 1306–9 (2009)

14. L. Bindi, J. M. Eiler, Y. Guan, L. S. Hollister, G. MacPherson, P. J. Steinhardt, N. Yao, "Evidence for the extraterrestrial origin of a natural quasicrystal," Proceedings of the National Academy of Sciences 109 (5): 1396–1401 (January 2012)
15. A. Gerlin, "Tecnion's Shechtman Wins Nobel in Chemistry for Quasicrystals Discovery," Bloomberg, (October 2011) available from: https://web.archive.org/web/20141205014945/http://www.bloomberg.com/news/2011-10-05/technion-s-shechtman-wins-chemistry-nobel-for-discovery-of-quasicrystals.html
16. P. J. Lu and P. J. Steinhardt "Decagonal and Quasi-crystalline Tilings in Medieval Islamic Architecture" Science 315 (5815): 1106–1110 (2007)
17. H. Wang, "Proving theorems by pattern recognition — II," The Bell System Technical Journal, vol. 40, no. 1, pp. 1-41, (Jan. 1961)
18. M. R. Robinson, "Undecidability and Nonperiodicity for Tilings of the Plane," Inventiones Mathematicae, vol. 12, p.177 (1971)
19. M. Gardner, "Penrose Tiles to Trapdoor Ciphers," Cambridge University Press (1997)
20. M. Gardner, The Second Scientific American Book Of Mathematical Puzzles and Diversions, "Phi:The Golden Ratio", Chapter 8, Simon & Schuster NY (1961)
21. C. Radin, "Book Review: Quasicrystals and geometry," Notices of the American Mathematical Society, 43 (4): 416–421 (April 1996)
22. Press release, NobelPrize.org, Nobel Media AB 2020, (October 1986) available from: https://www.nobelprize.org/prizes/physics/1986/press-release/
23. C. Bai, "Scanning tunneling microscopy and its applications," New York: Springer Verlag (2000)
24. I. Horcas et al., "WSXM: A software for scanning probe microscopy and a tool for nanotechnology," Review of Scientific Instruments 78, 013705 (2007)
25. M. T. Heideman, et al., "Gauss and the History of the Fast Fourier Transform," IEEE ASSP Magazine (Oct 1984)
26. WaveMetrics, "Igor 8 Brochure." (2018) available from: https://www.wavemetrics.net/Downloads/Igor8BrochureEnglish.pdf
27. R. Penrose, "Pentaplexity", Eureka, 39 (1978)

Figure 1a: https://commons.wikimedia.org/wiki/File:Zn-Mg-HoDiffraction.JPG

Figure 1b: https://commons.wikimedia.org/wiki/File:Ho-Mg-ZnQuasicrystal.jpg

Figure 2: https://commons.wikimedia.org/wiki/File:Penrose_Tiling_(P1).svg

Figure 9:
https://commons.wikimedia.org/wiki/File:Scanning_Tunneling_Microscope_schematic.svg

Figure 10: https://hemrajsharma.com/research/

7. Appendices

7.1. Data

Table 2: All the individually measured step heights from a collection of clean surface STM images.

Image	Step Height, Å	Step Type
1	2.549	S
	5.671	M
	10.56	L
	2.278	S
	2.517	S
	2.557	S
	2.239	S
	9.97	L
	8.025	L
	8.49	L
	4.765	M
	2.582	S
	6.834	M
	5.531	M
	10.12	L
	1.895	S
	8.495	L
	2.714	S
2	5.961	M
	2.895	S
	8.856	L=M+S
	5.156	M
	2.874	S
	8.03	L=M+S
	5.431	M

	2.947	S
	2.898	S
	2.242	S
	2.73	S
	5.853	M
	2.749	S
3	5.569	M
	2.222	S
	8.35	L
	2.898	S
	8.398	L
	2.717	S
	7.429	L
	2.522	S
4	2.823	S
	8.297	L
	2.55	S
	8.031	L
	5.564	M
	2.247	S
	2.788	S
5	5.647	M
	2.666	S
	8.22	L=M+S
	8.365	L
	2.194	S
	5.78	M
	5.43	M
6	2.226	S
	8.027	L
	8.505	L
	8.095	L
	5.82	M
	5.559	M

	4.653	M
7	5.491	M
	2.136	S
	5.476	M
	2.763	S
8	7.84	L
	2.601	S
	5.389	M
	2.558	S
9	2.948	S
TOTAL STEPS	69	

Table 3: The data from table 2 collated for each step type, this used to produce both table 1 and table 1a.

S	**M**	**L**
2.549	5.671	10.56
2.278	4.765	9.97
2.517	6.834	8.025
2.557	5.531	8.49
2.239	5.961	10.12
2.582	5.156	8.495
1.895	5.431	8.856
2.714	5.853	8.03
2.895	5.569	8.35
2.874	5.564	8.398
2.947	5.647	7.429
2.898	5.78	8.297
2.242	5.43	8.031
2.73	5.82	8.22
2.749	5.559	8.365
2.222	4.653	8.027
2.898	5.491	8.505

2.717	5.476	8.095
2.522	5.389	7.84
2.823		
2.55		
2.247		
2.788		
2.666		
2.194		
2.226		
2.136		
2.763		
2.601		
2.558		
2.948		

Table 1a: Corrected version of table 1, with the three largest L values discounted, causing the value calculated (here labelled L*) to be consistent with both the theoretical value and previously published value.

	S	**M**	**L***
total	31	19	16
avg	2.6	5.6	8.2
sd	0.28	0.45	0.34
error	0.051	0.1	0.085
Previous paper:			
given value	2.8	5.8	8.5
error	0.4	0.3	0.5
Model:			
given value	2.5	5.7	8.2
Paper:|A-B|	0.2	0.2	0.3
$3(a^2+b^2)^{0.5}$	1.2	0.95	1.5
	consistent	**consistent**	**consistent**
Model:|A-B|	0.1	0.1	0

$3(a^2+b^2)^{0.5}$	0.15	0.3	0.26
	consistent	**consistent**	**consistent**

Table 4: Demonstrating τ-sclaing by comparing the lines between opposite first and second order bright spots of an FFT. The ratio of the larger lines to the smaller is shown to be consistent with τ.

	first order disance, 1/nm	**second order disance, 1/nm**
	1.032	1.674
	1.081	1.75
	1.021	1.642
	0.914	1.479
	0.92	1.485
avg	0.9936	1.606
sd	0.073513944	0.119818613
error	0.032876435	0.053584513
τ	1.618033989	
d2/d1	1.616344605	
error d2/d1	0.075952128	
|τ-d2/d1|	0.001689383	**Consistent?**
3(error d2/d1)	0.227856383	Yes

Table 5: Pentagon lengths of the three images containing an Ag atom at the vertex of the pentagons that would form by Ag adsorption.

Frame	**Length, nm**
1	0.853
	1.082
	1.082

	0.999
	1.353
2	1.007
	0.93
	0.814
	1.375
	0.91
3	0.894
	1.156
	1.112
	1.091
	1.287
AVG	1.063
SD	0.174677
ERROR	0.045101

Table 6: Using the average value and error from table 5, they were checked for consistency against theoretical data and previously published data (for Bi)[7] and were found to be so.

		Length (nm)	**Error (nm)**
Theoretical Data:		1	0
Consistency Check:	$\lvert A-B \rvert$	0.063	
	$3(a^2+b^2)^{0.5}$	0.135304102	**consistent**
Previous Paper:		0.95	0.05
Consistency Check:	$\lvert A-B \rvert$	0.113	
	$3(a^2+b^2)^{0.5}$	0.202007921	**consistent**

7.2. Presentation Questions

Reviewer 1:

Question 1: At what temperature did you study the Ag motion on the quasicrystal surface, and is this an important variable to control?

The Ag deposition was at room temperature. Considering the growth of the thin film at different stages, this should be kept at the same temperature, to see clearly the way in which it forms. But the entire thin film growth could be at any temperature. There are some quasicrystals that destabilise at higher temperatures; fortunately the one used in this experiment is not one of those. There was other data taken at higher temperatures, but this was not deemed to be useful to this project, although there could be future work considering the difference of the thin film growth at different temperatures.

Question 2: Why was Ag chosen to decorate the surface, what other atoms would work well for the experiment?

Similar experiments have been done on this specific quasicrystal with lead and bismuth. The reason for these experiments is to create a thin film growth that has the same structure of the quasicrystal, but is more simple chemically (being comprised of only one element, instead of three), in order to explore the bulk properties of the structure. Silver was used this time simply because it hasn't been attempted before. There is also a previously published paper on the theory of how silver would adsorb onto this quasicrystal, so this project was testing the hypotheses in that paper. As for other atoms that could work, I would assume similar to those that have already been tried: those in the same group as bismuth, lead, and silver, such as antimony, tin, gold and copper.

Reviewer 2:

Question 1: What was the purpose of the FFT and what are you then looking at?

The FFT shows the quasicrystal in reciprocal space. This produces an image similar to the diffraction pattern shown by LEED. By selecting the bright spots and filtering the image, the surface of the quasicrystal is then recreated in real space, only using the selected points. As those points highlight the five-fold symmetrical nature of the surface of the quasicrystal, the filtered image produced shows this five-fold symmetrical nature much more clearly.

Question 2: Can you explain the process of using the STM and the purpose of switching the bias?

The STM uses an atomically sharp probe near the surface of the sample being scanned, then sending a current through, electrons tunnel from the probe through the sample, this creates a high resolution image of the surface of the sample. As the STM can be used with a negative or positive bias, this can effectively create two different images of the same area. This is because what is shown in the image produced by STM, depending on the bias, is the density of states. With the sample at positive bias, the unoccupied states of the sample are probed – at a negative sample bias; the occupied states of the sample are probed. When probing the surface of this quasicrystal, the Ag/In rings that are the vertices for the pentagonal tiling can be seen as protrusions at a negative bias. While at a positive bias, it is the Yb rings around the Ag/In that is resolved instead.

7.3. Project Proposal

PHYS379 BSc Project Proposal

Probing Atoms Using Scanning Tunnelling Microscopy

In this project, I will be considering the growth of metallic thin films on the surface of Ab-In-Yb quasicrystals, with the objective of creating a quasicrystalline Ag film. By learning, and utilising, the techniques of scanning tunnelling microscopy (STM) and low energy electron diffraction (LEED) I will be able to characterise the surface as well as the thin film growth on the crystal.

Being a relatively new area of materials science, as quasicrystals were only first observed in 1982, this leaves room for potentially large amounts of applications and utilisations. A lot of the groundwork is still being done in this area, which may lead us to many future discoveries. This project is a part of that groundwork. Without the characterisation of surfaces and the quasicrystalline thin film, we simply do not know how these materials may be used. Never before has a quasicrystalline film of Ag been characterised, and once this is done, then this can be compared with previously published theoretical calculations, and can then be utilised in further research in this area, such as finding applications for this quasicrystal, and possibly an important step in technological progress.

The film will be grown on an atom-by-atom basis using the thermal evaporation method. The resulting film will then be characterised by STM and LEED.

Density functional theory calculations reveal that Ag atoms are absorbed at specific atomic sites of the substrate, yielding a quasicrystalline structure. The experimental results will be compared with theoretical calculations published previously.

Once my project is complete, this work can then be further built upon, with new projects to suggest further test and experiments of this never before tested quasicrystal, potentially leading to interesting physical properties applicable to technological applications, as well as progression in field of materials science.

Timeline:

Week 1 – Research to gain familiarity in the background of the subject, as well as analysing software (WSxM) and LATEX.

Week 2 – Completion of background research, completion of paperwork, ready to begin project.

Week 3 to 6 – Experimental data collected over this period.

Week 5 onwards – Analysis of experimental data, begin on report.

Week 8 – Presentation given on how the experiment went, and discussion of preliminary findings.

Week 12 – End of project period, report completed.

7.4. Personal Reflection

It took me a few weeks to properly start my project. Fortunately, I left plenty of time in my project proposal at the start for background reading to accommodate this. The experimental data was already largely completed and given to me over weeks 4 and 5. I found starting the project quite interesting, as I've never looked into any materials science properly before, didn't know what a quasicrystal was until I started this project. So I found it fascinating reading through several academic papers to begin with. The underlying physics is not difficult to understand, so there wasn't a steep learning curve while getting to grips with the project. Even writing my presentation I made take longer than I needed, done over the space of a few days once the initial data analysis was done. Then I was given more data, without which there would be a lot less to talk about in my report, so I see that as a plus. Especially because the first draft just reached the minimum word count. I found that first draft quite a struggle to complete, being quite unmotivated over the Easter break, which was the time I set aside to do it. I did want there to be quite a large difference between my first and second draft, but the first draft took so much time, this was not possible, so the introductory sections were not as well researched as I would have liked. I would say overall that I enjoyed this project, learning something knew and seeing research at the forefront of a field. The only negative thing I have is that it took me so long to get a hang of the Penrose tiling, it was genuinely infuriating, and they can still be made better.